Langmuir

Article

pubs.acs.org/Langmuir

# Strain-Controlled Switching of Hierarchically Wrinkled Surfaces between Superhydrophobicity and Superhydrophilicity

Zuoqi Zhang,[†] Teng Zhang,[‡] Yong Wei Zhang,[†] Kyung-Suk Kim,[‡] and Huajian Gao*[,‡]

[†]Department of Engineering Mechanics, Institute of High Performance Computing, A*STAR, Singapore, 138632, Singapore

[‡]School of Engineering, Brown University, Providence, Rhode Island 02912, United States

Supporting Information

**ABSTRACT:** Recent years have witnessed intense interest in multifunctional surfaces that can be designed to switch between different functional states with various external stimuli including electric field, light, pH value, and mechanical strain. The present paper is aimed to explore whether and how a surface can be designed to switch between superhydrophobicity and superhydrophilicity by an applied strain. Based on well-established theories of structure buckling and solid−liquid contact, we show that this objective may be achieved through a hierarchically wrinkled surface. We derive general recursive relations for the apparent contact angle at different levels of the hierarchical surface and investigate the thermodynamic stability of different contact states. Our study may provide useful guidelines for the development of multifunctional surfaces for many technological applications.

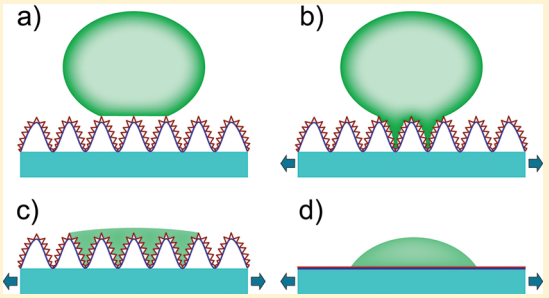


## 1. INTRODUCTION

Multifunctional surfaces switchable between superhydrophobicity and superhydrophilicity, if proven feasible, would stimulate broad applications in modern technology ranging from water harvesting,[1−3] oil spill cleanup,[4−6] reversible adhesion,[7−10] self-cleaning,[11−14] environmental cleanup,[15,16] microfluidics,[17−19] micro- and nanofabrication,[20] robotics,[21,22] energy conversion,[23,24] and biomedical engineering.[25] In this context, it is especially interesting to observe that gecko's feet constitute a multifunctional hierarchical system that exhibits superhydrophobicity, nonstickiness, and self-cleaning at its default state, while easily and reversibly switchable to a strongly sticky state by scratching/sliding against a substrate.[26−29] In contrast, most manmade systems today could focus on only one particular function, for example, wettability[30,31] or adhesion.[32−35] Some existing studies have involved electrochemically switchable wetting/antiwetting states. For example, Xia et al. reported dual-responsive surfaces that can be switched between superhydrophilicity and superhydrophobicity by varying temperature and/or pH value;[36] Lim et al. demonstrated a photoreversibly switchable superhydrophobic surface via a nanoporous multilayer film modified with a photoswitchable agent;[37] Riskin et al. showed some biocatalytically or electrochemically switchable interfacial properties of $Ag^+$-biphenyldithiol monolayers associated with a Au surface.[38] In addition, there are also some attempts to develop mechanically tunable topographically corrugated surfaces for specific functions such as marine antifouling and self-cleaning. Efimenko and co-workers developed a three-step method to fabricate hierarchically wrinkled artificial skins by first stretching PDMS sheets, then applying ultraviolet/ozone (UVO) treatment to densify and stiffen their upper surfaces, then gradually releasing the prescribed strain, and finally generating hierarchically wrinkled skins.[39] In subsequent work, the developed hierarchically wrinkled artificial skins have been tested for marine antifouling.[16] In this method, the wavelength at each hierarchical level is critically determined by the material adopted. Lin et al. realized mechanically switchable wetting on wrinkled elastomers with coated nanoparticles, but their design was only able to raise the contact angle from 112° to 150°,[20] and did not take controllable adhesion into consideration. Gecko inspired reversible adhesives have been intensively studied in the literature recently.[12,21,22,40−44] In spite of this progress, the important question regarding whether and how a surface could be designed to be switchable between superhydrophobicity and superhydrophilicity by an applied strain remains unanswered. Here, we show that this can be achieved through a hierarchically wrinkled surface.

It is well-known that wettability and adhesion of a surface is governed not only by its chemical compositions, but also by surface topography.[45−50] Lotus leaf is a well-known example of a surface achieving superhydrophobicity, low adhesion, and self-cleaning (also known as the Lotus effect) with a two-level hierarchical surface structure.[51] Since sophisticated surface morphology can now be fabricated and altered with mechanical strain,[39,52−59] the time is now ripe to explore mechanically switchable multifunctional surfaces more thoroughly. Figure 1 shows the basic idea and applications of using various external stimuli including mechanical strain to control surface topography to tune wetting and adhesion properties of a surface.

**Received:** October 7, 2011
**Revised:** December 15, 2011
**Published:** December 16, 2011

   dx.doi.org/10.1021/la203934z | *Langmuir* 2012, 28, 2753−2760

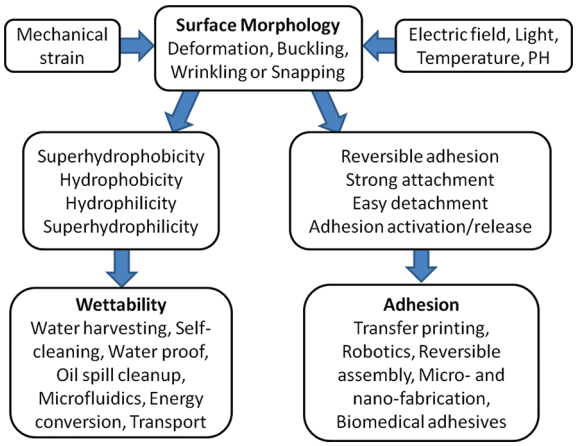


**Figure 1.** Potential applications of tunable multifunctional devices via control of surface morphology through external stimuli including mechanical strain.

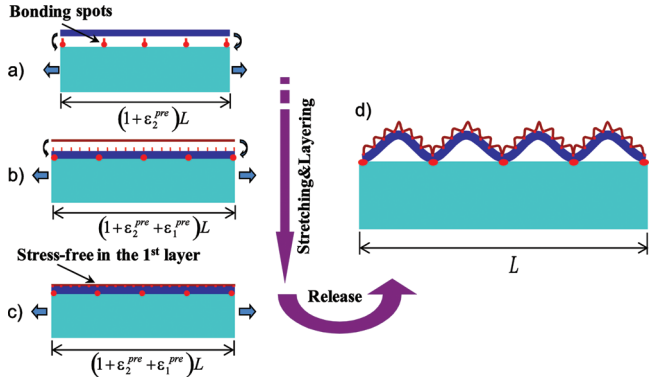


**Figure 2.** A "stretch-and-release" layer fabrication route for a substrate-supported hierarchically wrinkled surface aimed at strain-controlled switching between superhydrophobicity and superhydrophilicity. The process consists of consecutively bonding a new layer at periodic binding sites (red dots) on a prestretched substrate consisting of previously bonded layers and the original substrate, as shown in (a)−(c) for a two-level wavy surface. The prestrain can then be released to buckle the attached layers to create a hierarchically wrinkled structure shown in (d). The procedure could be repeated to create an *n*-level wavy surface.

In this paper, we consider the wettability of a hierarchically wrinkled surface with sinusoidal waviness on several length scales, which can be mechanically tuned between superhydrophilicity and superhydrophobicity by an applied strain. We will utilize the well-established theories of structural buckling and solid−liquid contact to explore the feasibility to design a hierarchically wrinkled surface that can be switched between superhydrophobic, hydrophobic, hydrophilic, and superhydrophilic regimes by an applied strain.

The paper is outlined as follows. Section 2 discusses the design and fabrication of a hierarchically wrinkled surface from stepwise buckling of a multilayered structure under mechanical strain. The relationship between such a hierarchical surface and its wetting properties is studied in section 3. Section 4 presents several examples and discussions to demonstrate that it is indeed possible to design hierarchically wrinkled surfaces that can reversibly switch between superhydrophobicity and superhydrophilicity. A summary of major conclusions are presented in section 5.

## 2. STRAIN-CONTROLLED DESIGN OF A HIERARCHICALLY WRINKLED SURFACE

Wrinkling, buckling, and other mechanical instabilities are widely utilized to generate/design a variety of patterns of surface roughness, as reviewed in a recent paper by Genzer and Groenewold.[59] To illustrate the basic principles involved, let us consider a thin layer bonded to a substrate which has been prestretched to a strain $\varepsilon_{pre}$. It is now well-established that releasing the prestrain would buckle the layer.[53,56,60−62] The resulting sinusoidal wavy surface has a wavelength that depends on the modulus ratio of the layer and substrate as $\lambda = 2\pi t(\bar{E}_f/3\bar{E}_s)^{1/3}$, where $t$ denotes the thickness of the layer, and $\bar{E}_f$ and $\bar{E}_s$ are the plane strain moduli of the layer and substrate, respectively. Note that the range of wavelength achieved through such spontaneous buckling of fully bonded films is limited by the Young's modulus ratio of materials available. In order to remove the limit on the achievable wavelength, in the present paper we adopt an alternative design that involves partially bonded films, allowing for a more flexible design of buckling-induced wrinkle patterns to meet the requirements for particular functions.

Figure 2 shows a possible route of fabrication for a two-level wavy surface, which can be repeatedly applied to generate an *n*-level wavy surface. In this design, a layer of material is attached to the prestretched substrate at a periodical array of bonding sites whose spacing is selected according to the desired wavelength at each hierarchical level. When new layers are attached subsequently, the prestrain in the substrate is incrementally increased according to the desired buckling amplitude of the added layer. Let $\lambda_i$ denote the spacing between the bonding sites at the $i$th hierarchical level, $\varepsilon_i^{pre}$ the incremental prestrain in the substrate when the $i$th layer is attached and $t_i$ the thickness of the $i$th layer which is assumed to decrease with each added level of hierarchy. After all layers are bonded, the strain in the substrate is gradually released to produce a hierarchically wavy surface of *n*-level. For buckling of this type, it has been shown that the amplitude of wrinkling is related to the $i$th prestrain increment $\varepsilon_i^{pre}$ as[39,53,56,60−62]

$$A_i = \frac{\sqrt{3}\,t_i}{3}\sqrt{\frac{\varepsilon_i^{pre}}{\varepsilon_i^c} - 1} \tag{1}$$

where $\varepsilon_i^c = (1/12)(k_i t_i)^2$ is the critical buckling strain and $k_i = 2\pi/\lambda_i$ is the wavenumber at the $i$th level. Normalizing this amplitude by the wavenumber gives

$$\tilde{A}_i = k_i A_i = 2\sqrt{\varepsilon_i^{pre} - \varepsilon_i^c} \tag{2}$$

The resulting *n*-level wavy surface can be reversibly wrinkled and flattened by applying an external strain $\varepsilon_{app}$ of different magnitude. At a given strain level $\varepsilon_{app}$, the amplitude of the $i$th layer is

$$\tilde{A}_i = k_i A_i = \begin{cases} 0 & \text{if } \varepsilon_{app} > \sum_{j\geq i} \varepsilon_j^{pre} - \varepsilon_i^c \\ 2\sqrt{\sum_{j\geq i} \varepsilon_j^{pre} - \varepsilon_{app} - \varepsilon_i^c} & \text{if } \sum_{j\geq i+1} \varepsilon_j^{pre} - \varepsilon_i^c < \varepsilon_{app} < \sum_{j\geq i} \varepsilon_j^{pre} - \varepsilon_i^c \\ 2\sqrt{\varepsilon_i^{pre} - \varepsilon_i^c} & \text{if } \varepsilon_{app} < \sum_{j\geq i+1} \varepsilon_j^{pre} - \varepsilon_i^c \end{cases} \tag{3}$$


dx.doi.org/10.1021/la203934z | *Langmuir* 2012, 28, 2753−2760

## 3. WETTABILITY AND ADHESION OF AN *N*-LEVEL WAVY SURFACE

Previous studies in the literature have addressed the effect of surface topography on wettability.[45−47] Here, we investigate how to control the wetting/antiwetting properties of a hierarchically wrinkled surface. We will build upon and extend the classical model and analysis by Herminghaus (2000).[47] Using a homogenization and iterative scheme, Herminghaus proposed a recursive approach (see eq 3 in Herminghaus' paper) to determine the effect of hierarchical surface roughness on the apparent contact angle, and mathematically deduced that a hierarchical roughness may render any surface with nonzero intrinsic contact angle nonwet, i.e., having an apparent contact angle close to 180°.[47] To illustrate Herminghaus' approach, consider an *n*-level wavy surface, as shown in Figure 2. The coordinates associated with the *i*th level are set up such that the surface profile of the *i*th hierarchy is

$$y_i = -A_i \cos(k_i x_i) \qquad i = 1, ..., n \tag{4}$$

The condition for achieving the Cassie state of having an overhung liquid on the wrinkled surface is that there exists a stable solid−liquid−air triple-junction $x_i = a_i$ which satisfies

$$\tilde{A}_i \sin \tilde{a}_i = \tan(\pi - \theta_{i-1}) \quad \tilde{a}_i \in (0, \pi] \qquad i = 1, ..., n \tag{5}$$

where $\tilde{a}_i = k_i a_i$ is the normalized coordinate and $\theta_{i-1}$ is the apparent contact angle on the $(i-1)$-th surface, $\theta_0$ being the intrinsic contact angle. If eq 5 cannot hold for a finite $0 < \tilde{a}_i \le \pi$, there will not be an equilibrium overhang and a Wenzel state would prevail with $\tilde{a}_i = 0$. Once $\tilde{a}_i$ is determined from eq 5, the apparent contact angle $\theta_i$ at the *i*th level can be expressed in terms of $\theta_{i-1}$ as (see Supporting Information)

$$\cos \theta_i = \frac{1}{\pi} \int_{\tilde{a}_i}^{\pi} \sqrt{1 + \tilde{A}_i^2 \sin^2 \tilde{x}_i}\, d\tilde{x}_i \cos \theta_{i-1} - \frac{\tilde{a}_i}{\pi}$$
$$i = 1, ..., n \tag{6}$$

where $\tilde{x}_i = k_i x_i$ is the normalized coordinate at the *i*th level. According to eqs 5 and 6, if one starts with a surface in a Wenzel state, i.e., $\theta_0 \le 90°$ and $\tilde{a}_1 = 0$, it will follow that $\cos \theta_1 \ge 0$ and $\tilde{a}_2 = 0$, $\cos \theta_2 \ge 0$ and $\tilde{a}_3 = 0$, and then, $\cos \theta_i \ge 0$ and $\tilde{a}_{i+1} = 0$ for all $i = 1, ..., n$, i.e., the surface will remain in the Wenzel state ($\tilde{a}_i \equiv 0$) at all levels regardless of the value of $\tilde{A}_i$ and *n*. Therefore, the recursive model based on homogenization and iteration alone would predict that it is impossible for a chemically hydrophilic surface to achieve hydrophobicity via surface roughness. This is neither consistent with experimental observations[63−65] nor with Herminghaus' deduction from a convergence analysis. Apparently, a more accurate modeling approach is needed to model the wettability of a hierarchically wrinkled surface, which should properly account for the overhang of a liquid drop on a hierarchical rough surface.

To address the overhang of a liquid drop (Cassie state) on a hierarchically wrinkled surface whose chemical composition is hydrophilic, here we adopt a geometrically exact approach. Assuming that the overhang starts from the *m*th level and persists to all higher levels, the critical condition for initiating the overhang in a geometrically exact model is to have $\tilde{a}_m = k_m a_m$ satisfy (see Supporting Information)

$$\sum_{j=1}^{m-1} \arctan(\tilde{A}_j) + \arctan(\tilde{A}_m \sin \tilde{a}_m) = \pi - \theta_0 \tag{7}$$

where $\theta_0 \le 90°$ is the contact angle of the material at the first hierarchy. The apparent contact angle at the *m*th level can be calculated from (see Supporting Information)

$$\cos \theta_m = \frac{1}{\pi} \int_{\tilde{a}_m}^{\pi} \sqrt{1 + \tilde{A}_m^2 \sin^2 \tilde{x}_m}\, d\tilde{x}_m \times \left[ \prod_{j=1}^{m-1} \left( \frac{1}{\pi} \int_0^{\pi} \sqrt{1 + \tilde{A}_j^2 \sin^2 \tilde{x}_j}\, d\tilde{x}_j \right) \right] \times \cos \theta_0 - \frac{\tilde{a}_m}{\pi} \tag{8}$$

Note that eq 7 is necessary but not sufficient for achieving the overhang, since interference between neighboring asperities may put off its occurrence. However, as shown in the Supporting Information, through proper design, it is possible to find a regime where no interference exists between neighboring asperities so that eq 7 becomes necessary and sufficient for the occurrence of the overhang. Once the overhang occurs, the Herminghaus recursive model can be adopted to simplify the scaleup analysis.

To investigate the stability of the Cassie state induced by surface roughness, we calculate the critical pressure for the reverse Cassie-to-Wenzel (CTW) transition. A detailed discussion is given in the Supporting Information. The main results are briefly summarized below. Following the Herminghaus recursive model, the *i*th level surface is represented as a sinusoidal surface with an effective contact angle $\theta_{i-1}$ calculated from the $(i-1)$th level, with its critical pressure determined from

$$\left.\begin{aligned} \frac{\partial \tilde{G}_i \langle \tilde{a}_i, \tilde{p}_i | \theta_{i-1} \rangle}{\partial \tilde{a}_1} &= 0 \\ \frac{\partial^2 \tilde{G}_i \langle \tilde{a}_i, \tilde{p}_i | \theta_{i-1} \rangle}{\partial \tilde{a}_i^2} &= 0 \end{aligned}\right\} \tag{9}$$

where $\tilde{G}_i = k_i G_i/(2\pi\gamma_{LA})$ and $\tilde{p}_i = p/(k_i\gamma_{LA})$ are, respectively, the dimensionless Gibbs free energy and liquid pressure at the *i*th level, and $\gamma_{LA}$ is the liquid/air interfacial energy. For the geometrically exact model, the maximum critical pressure occurs at $\tilde{a}_2, ..., \tilde{a}_m = \pi/2$, and can be determined from the following equations

$$\left.\begin{aligned} \frac{\partial \tilde{G}_m \left\langle \tilde{a}_1, \tilde{p}_m \middle| \tilde{a}_2, ..., \tilde{a}_m = \frac{\pi}{2}, \theta_0 \right\rangle}{\partial \tilde{a}_1} &= 0 \\ \frac{\partial^2 \tilde{G}_m \left\langle \tilde{a}_1, \tilde{p}_m \middle| \tilde{a}_2, ..., \tilde{a}_m = \frac{\pi}{2}, \theta_0 \right\rangle}{\partial \tilde{a}_1^2} &= 0 \end{aligned}\right\} \tag{10}$$

in which $\tilde{G}_m = (k_m G_m)/(2\pi\gamma_{LA})$ is the normalized Gibbs energy of the wavy surface with *m* levels of hierarchy while $\tilde{p}_m = p/(k_m\gamma_{LA})$ is the normalized liquid pressure at the *m*th level.


dx.doi.org/10.1021/la203934z | Langmuir 2012, 28, 2753−2760

As the surface is switched between hydrophilicity and hydrophobicity, especially between superhydrophilicity and superhydrophobicity, via hierarchical waviness, the capillary adhesion property of the surface also changes substantially. To see this, let us define the contact area fraction as the ratio of real contact area over the total surface area. For a liquid on an $n$-level wavy surface, the contact area fraction can be expressed as

$$\tilde{S} = \prod_{i=1}^{n} \left( \int_{\tilde{a}_i}^{\pi} \sqrt{1 + \tilde{A}_i^2 \sin^2 \tilde{x}_i}\, d\tilde{x}_i / \int_0^{\pi} \sqrt{1 + \tilde{A}_i^2 \sin^2 \tilde{x}_i}\, d\tilde{x}_i \right) \quad (11)$$

The real contact area for a liquid suspended on a multiscale wavy surface ($\tilde{A}_i > 0$) is generally several orders smaller in magnitude than that on a flat surface ($\tilde{A}_i = 0$).[66] The real contact area could be even smaller for the wavy surface against a flat solid substrate. Thus, the contact area can be altered in a wide range as the hierarchical wavy surface is gradually flattened under stretching.

## 4. RESULTS AND DISCUSSION

Combining the results of sections 2 and 3, we can investigate the properties of a hierarchically wrinkled surface by taking proper system parameters. Figure 3a shows a Cassie-superhydrophobic state at the default ($\varepsilon_{app} = 0$), with Lotus-type self-cleaning characteristics. Given a certain value of the applied strain $\varepsilon_{app}$, the surface would become Wenzel-superhydrophobic (Figure 3b) if it is chemically hydrophobic ($\theta_0 > 90°$) and superhydrophilic (Figure 3c) if it is chemically hydrophilic ($\theta_0 < 90°$). Figure 3d shows that the real contact area can dramatically increase as the surface is completely flattened by the applied strain. To demonstrate the change in functional states of the hierarchically wrinkled surface under different applied strain levels, three examples of design are discussed in this section.

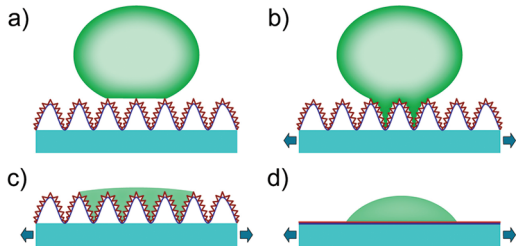


**Figure 3.** Illustration of different functional states of a hierarchically wrinkled surface under applied strain. (a) At the default state, the surface is in a Cassie-type superhydrophobic and self-cleaning state; under stretching, the surface becomes (b) Wenzel-superhydrophobic if it is chemically hydrophobic ($\theta_0 > 90°$) or (c) superhydrophilic if it is chemically hydrophilic ($\theta_0 < 90°$); (d) the real contact area can increase dramatically as the surface is completely flattened.

The first example is a surface designed to achieve superhydrophobicity ($\theta$>150°) from a hydrophobic material ($\theta_0 >$ 90°) via two-scale wavy surface, similar to Lotus leaves.[11,51] In this example, a chemically hydrophobic surface is chosen with contact angle $\theta_0 = 120°$, and the surface tension of water is set at $\gamma_{LA} = 0.073$ J/m$^2$. The structural parameters are taken as $\lambda_1 = 100$ nm, $\lambda_2 = 10$ $\mu$m, and correspondingly $k_1 = 6.2832 \times 10^7$ m$^{-1}$, $k_2 = 6.2832 \times 10^5$ m$^{-1}$. Both the material wettability and the structural size are chosen to be close to those of the Lotus leaves ($\theta_0 \approx 110°$, $\lambda_1 \approx 100$ nm, $\lambda_2 \approx 10-50$ $\mu$m).[11,51,67] The thicknesses of the bonded layers are selected as $t_i = \lambda_i/10$ ($i$ = 1, 2) so that the critical strain for buckling is kept at $\varepsilon_i^c = (1/12)(k_i t_i)^2 = 0.03$ ($i$ = 1, 2). As shown in Figure 2, application of prestrains $\varepsilon_1^{pre} = \varepsilon_2^{pre} = 0.94$ during sequential attachment of two layers and then releasing the prestrains lead to a self-similar two-level wavy surface with dimensionless amplitudes $\tilde{A}_1 = \tilde{A}_2 =$ 1.91. From eqs 3−9, the apparent contact angle $\theta$, the triple-junction position $\tilde{a}$, the critical pressure $\tilde{P}_{CTW}$ for the CTW transition and the contact area fraction are plotted against the applied strain in Figure 4a−d, respectively. It can be seen that, at the relaxed state ($\varepsilon_{app} = 0$), a strong Cassie-superhydrophobic state ($\theta = 174°$, with $k_2 a_2 = 2.885$ and $\tilde{S} =$ 0.0168; also see Figure 3a) is achieved through the two-level wavy structure, in which case the surface is self-cleaning like Lotus leaves. The absolute value of the CTW pressure is calculated to be $p_2^{CTW} = 0.0279$ MPa at the top (micro) level, and $p_1^{CTW} = 0.120$ MPa at the bottom (nano) level. Since $p_2^{CTW}$ is larger than 146 Pa, the static pressure induced by the surface tension of a water drop of 2 mm[66] and $p_1^{CTW}$ is larger than 0.1 MPa, the extreme pressure found in nature coming from the impact by water droplets in a rainfall,[68] the two-level surface is robust enough for self-cleaning in a natural environment. Note that the structural hierarchy also makes the superhydrophobic state more easily restorable from the Wenzel state via disturbances such as wind or slight mechanical vibrations,[66,69] which guarantees the repeatability and reversibility of the multifunctional surface. As the applied strain increases, the apparent contact angle, the liquid/air/solid triple junction, and the CTW pressure all decline, as shown in Figure 4a−c, respectively, while the contact area fraction increases as shown in Figure 4d. As $\varepsilon_{app}$ reaches the second regime $0.85 \le \varepsilon_{app} <$ 0.91, the wetting state abruptly changes from a superhydrophobic state with both levels remaining in the Cassie state (as shown in Figure 3a) to a superhydrophobic state ($\theta > 150°$) with the lower level remaining in the Cassie state ($k_1 a_1 > 0$), but the higher level shifted to a Wenzel state ($k_2 a_2 > 0$, as shown in Figure 3b). As $\varepsilon_{app}$ exceeds $\varepsilon_2^{pre} - \varepsilon_2^c = 0.91$, the microscale roughness disappears according to eq 3, and the surface remains weakly superhydrophobic with $\theta$ slightly larger than 150° via a Cassie state ($1.616 \le k_1 a_1 \le 2.000$ and $0.3236 \le \tilde{S} \le 0.4816$) until $\varepsilon_{app} = 1.1$. As the applied strain continues to rise beyond $\varepsilon_{app} = 1.1$, the surface becomes normally hydrophobic ($120° \le \theta \le 150°$) in a Wenzel state ($k_1 a_1 = 0$ and $\tilde{S} = 1$). When $\varepsilon_{app}$ exceeds $\sum_{j \ge 1}^{2} \varepsilon_j^{pre} - \varepsilon_1^c = 1.85$, the nanoscale roughness snaps to a completely flat substrate (as shown in Figure 3d). To some extent, our design is consistent with experiments by Lin and Yang who reported mechanically switchable wetting on wrinkled elastomers with dual-scale roughness.[20] Since Lin and Yang coated rippled PDMS with nanoparticles to form dual-scale roughness, their nanoscale roughness was not mechanically controllable. Moreover, the apparent contact angle was mechanically tunable from 150° (slightly superhydrophobicity) to 128° in their experiment, which is smaller than the predicted range from 174° to 120° in our calculations.

As the second example, a self-similar three-scale wavy surface is designed with tunable wettability from slightly hydrophilic


dx.doi.org/10.1021/la203934z | Langmuir 2012, 28, 2753−2760

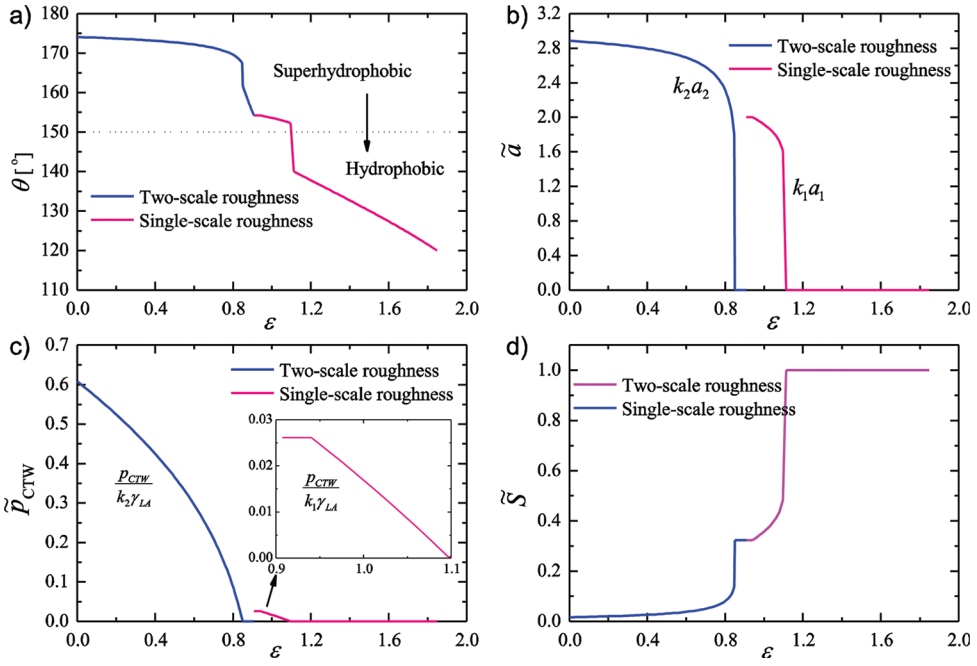


**Figure 4.** Two-scale wavy surface designed for tunable wettability from hydrophobicity to strong superhydrophobicity: (a) apparent contact angle varying with respect to the applied strain; (b) position of liquid/air line versus the applied strain; (c) dimensionless pressure for CTW transition over the applied strain; and (d) contact area fraction varies with respect to the applied strain.

($\theta_0 = 80°$) to strongly superhydrophobic ($\theta = 169°$), with parameters selected as follows:

$$\theta_0 = 80°,\ \gamma_{LA} = 0.073\ \mathrm{J/m^2};$$

$$\lambda_1 = 100\ \mathrm{nm},\ \lambda_2 = 1\ \mu\mathrm{m},\ \lambda_3 = 10\ \mu\mathrm{m} \Rightarrow$$

$$k_1 = 6.2832 \times 10^7\ \mathrm{m^{-1}},\ k_2 = 6.2832 \times 10^6\ \mathrm{m^{-1}},\ k_3 = 6.2832 \times 10^5\ \mathrm{m^{-1}};$$

$$t_i = \frac{\lambda_i}{10} \Rightarrow \varepsilon_i^c = 0.03,\ i = 1, 2, 3;\ \varepsilon_i^{pre} = 0.7980 \Rightarrow \tilde{A}_i = 1.75,\ i = 1, 2, 3$$

As the applied strain increases, Figure 5 shows the apparent contact angle (panel a), the movement of liquid/air line (panel b), the dimensionless pressure for the CTW transition (panel c), and the contact area fraction (panel d). It can be concluded that the relaxed state ($\varepsilon_{app} = 0$) is strongly Cassie-superhydrophobic ($\theta = 169°$ with $k_3a_3 = 2.690$ and $\tilde{S} = 0.0114$) and self-cleaning (as in Figure 3a). The CTW pressure is calculated to be $p_3^{CTW} = 0.0146$ MPa at the third level, 2 orders of magnitude higher than the typical static pressure of a water drop 146 Pa. The transition from hydrophilicity to hydrophobicity, $\theta_0 = 80° \rightarrow \theta_2 = 143°$, is achieved by the bottom two levels of the wavy structure since the liquid is overhung on the nanoscale roughness at $k_2a_2 = 2.646$, according to eqs 7 and 8. From eq 10, the CTW pressure of the overhang state is found to be $p_2^{CTW} = 0.116$ MPa, which is slightly larger than the rainfall pressure 0.1 MPa. When $\varepsilon_{app}$ becomes larger than 0.62, the self-cleaning state shown in Figure 3a comes to an end and transits into a weakly Wenzel-superhydrophobic state ($k_3a_3 = 0$ but $k_2a_2 > 0$, as in Figure 3b) until $\varepsilon_{app} = \varepsilon_3^{pre} - \varepsilon_3^c = 0.765$, after which the third level of waviness is flattened. In the regime of $0.765 \le \varepsilon_{app} < 1.387$, the remaining two-scale roughness is still hydrophobic; when $\varepsilon_{app} \ge 1.387$, the two-scale roughness can no longer carry the overhanging liquid and the surface slips into hydrophilic regime. When $\varepsilon_{app}$ exceeds $\sum_{j\ge 2}^{3}\varepsilon_j^{pre} - \varepsilon_2^c = 1.563$, the second level of waviness disappears. In the end, the surface becomes completely flat when $\varepsilon_{app} \ge \sum_{j\ge 1}^{3}\varepsilon_j^{pre} - \varepsilon_1^c = 2.361$. It has been reported that mushroom-shaped microfiber arrays made from hydrophilic polyurethane with a contact angle 82° showed an apparent contact angle of 128°, in which microfibers and mushroom-shaped tips effectively acted as two-scale roughness.[64]

A three-scale wavy surface with tunable wettability covering hydrophilic ($\theta_0 = 60°$) to strongly superhydrophobic ($\theta = 161°$) and to superhydrophilic ($\theta < 5°$) states is demonstrated in the third example of design. The following parameters are adopted:

$$\theta_0 = 60°,\ \gamma_{LA} = 0.073\ \mathrm{J/m^2};$$

$$\lambda_1 = 100\ \mathrm{nm},\ \lambda_2 = 1\ \mu\mathrm{m},\ \lambda_3 = 10\ \mu\mathrm{m} \Rightarrow$$

$$k_1 = 6.2832 \times 10^7\ \mathrm{m^{-1}},\ k_2 = 6.2832 \times 10^6\ \mathrm{m^{-1}},\ k_3 = 6.2832 \times 10^5\ \mathrm{m^{-1}};$$

$$t_i = \frac{\lambda_i}{10} \Rightarrow \varepsilon_i^c = 0.03,\ i = 1, 2, 3;$$

$$\varepsilon_1^{pre} = \varepsilon_2^{pre} = 1.60,\ \varepsilon_3^{pre} = 0.90 \Rightarrow \tilde{A}_1 = \tilde{A}_2 = 2.50,\ \tilde{A}_3 = 1.86$$

Figure 6 shows the varying apparent contact angle over the applied strain (panel a), the movement of liquid/air line with respect to the applied strain (panel b), the dimensionless pressure for CTW transition over the applied strain (panel c), and the contact area fraction versus the applied strain (panel d). As can be seen from Figure 6, the relaxed state ($\varepsilon_{app} = 0$) is strongly Cassie-superhydrophobic ($\theta = 161°$ with $k_3a_3 = 2.412$ and $\tilde{S} = 0.0192$). The CTW pressure is calculated to be $p_3^{CTW} =$ 5.96 KPa at the third scale, which is significantly larger than the


dx.doi.org/10.1021/la203934z | Langmuir 2012, 28, 2753−2760

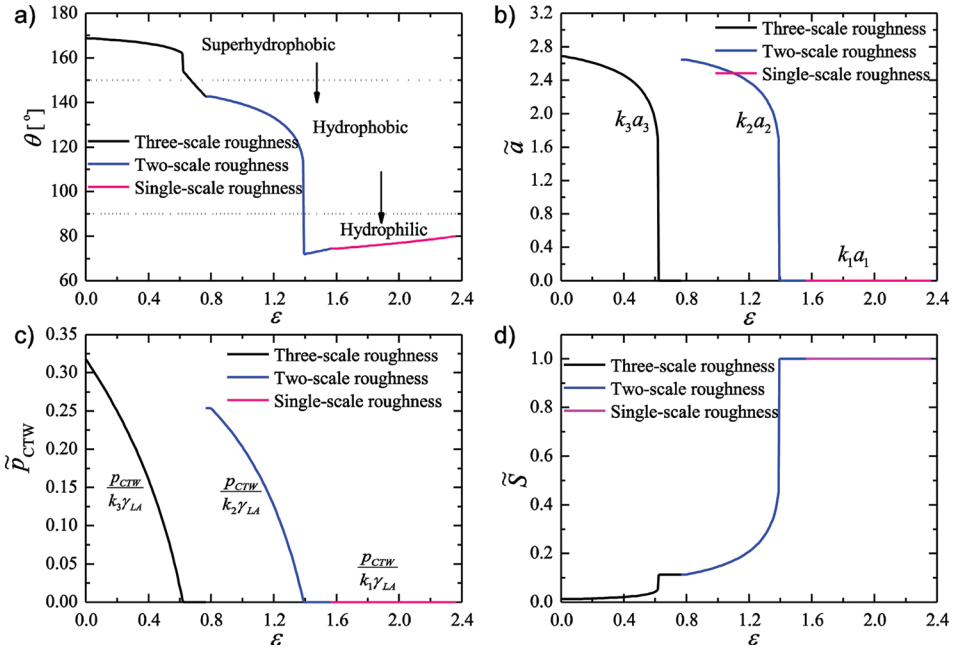


**Figure 5.** Properties of a three-scale wavy surface designed for tunable wettability from slightly hydrophilicity to strong superhydrophobicity. (a) The varying apparent contact angle; (b) the movement of liquid/air line; (c) the dimensionless pressure for CTW transition; and (d) the contact area fraction varies with respect to the applied strain.

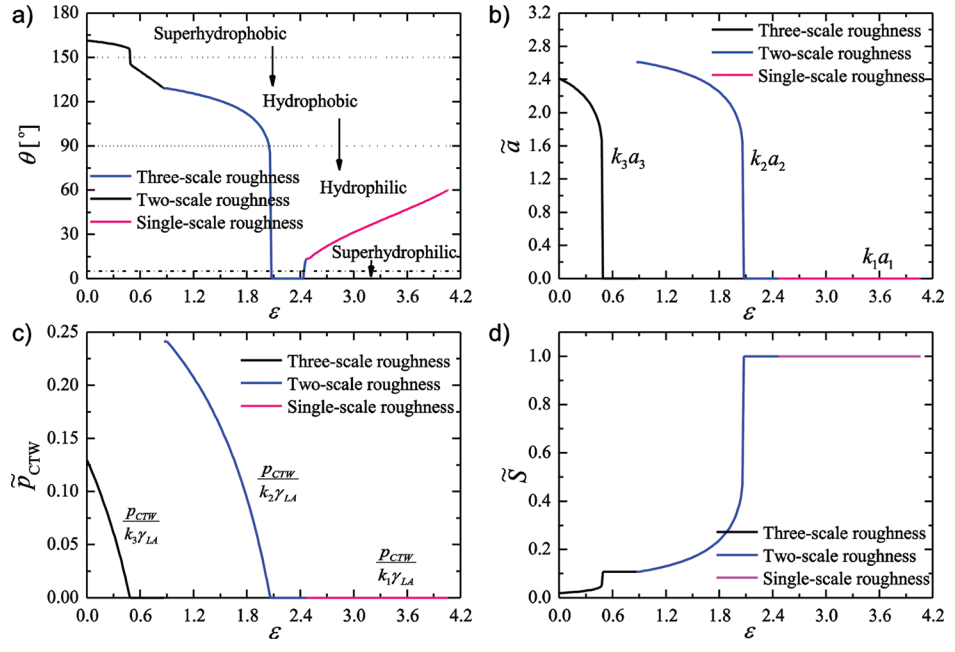


**Figure 6.** Properties of a three-scale wavy surface designed for tunable wettability from superhydrophilicity to superhydrophobicity: (a) varying apparent contact angle; (b) movement of liquid/air line; (c) dimensionless pressure for CTW transition; and (d) contact area fraction versus applied strain.

typical static pressure 146 Pa of a liquid drop, while $p_2^{CTW}$ = 0.111 MPa at the second scale is larger than the typical rainfall pressure of 0.1 MPa. As the applied strain increases, the variation of the apparent contact angle, the liquid/air line, the CTW pressure and the contact area fraction can be separated into several regimes as shown in Figure 6a–d. In the regime of $\varepsilon_{app} < 0.480$, the surface with three-scale roughness is in a Cassie-superhydrophobic, low adhesion, and self-cleaning state; For $0.480 \leq \varepsilon_{app} < 0.870$, the Cassie state is replaced by a Wenzel state, and the surface becomes normally hydrophobic; when $0.870 \leq \varepsilon_{app} < 2.059$, the third level roughness is flattened, but the two-scale roughness can still carry an overhanging liquid drop and the surface is still hydrophobic; in the regime $2.059 \leq \varepsilon_{app} < 2.466$, the two-scale roughness can no longer carry an overhanging liquid drop and turns to promote the hydrophilicity through a Wenzel state, resulting in superhydrophilicity; when $2.466 \leq \varepsilon_{app} < 4.061$, only single-scale wavy structure remains, and the surface becomes completely flat


dx.doi.org/10.1021/la203934z | Langmuir 2012, 28, 2753–2760

at the end. We can see that a mechanically controlled switch from superhydrophobicity to superhydrophilicity is realized by this design which, to our best knowledge, has not been previously reported in the literature.

The main objective of our present work is to investigate the existence of hierarchically wrinkled surfaces capable of switching between superhydrophobicity and superhydrophilicity by an applied strain. Our preliminary analysis indicates that, while possible in principle, the ability to switch from superhydrophilic to superhydrophobic using surface wrinkling may require rather complex fabrication schemes. In several aspects, our work is very preliminary and needs to be tested experimentally. Below are a number of issues worth further investigation:

(1) There exist discrepancies between the assumed sinusoidal shape of a wrinkled film in section 2 and large-amplitude bucking shape of the film at strain levels as large as 200−400%. These discrepancies may affect the required values of both the prestrain during fabrication and the applied strain for functionality switching, although the buckling induced wavy structure should remain a fundamental feature.[53,56,60,62,70] More sophisticated theories taking into account large deformation and nonlinear elasticity can be introduced to fine-tune specific designs in the future work, but they should not affect the basic concepts involved.

(2) Further study is needed to account for the reverse transition of a liquid drop on a hierarchically wrinkled surface from wetting (Wenzel state) to nonwetting (Cassie state). As stressed and rationalized by Herminghaus, a hierarchical wrinkled surface may be completely dry or completely wet depending on the history, and its liquid-repellent property is not an equilibrium property.[47] If a liquid drop starts in a Wenzel state on a flat surface which subsequently develops a hierarchical wrinkled topography, the drop may remain in a metastable Wenzel state without spontaneously transitioning into a Cassie state. However, it has been theoretically[66] and experimentally[69] shown that nano to micro structural hierarchy on Lotus leaves makes the Cassie state easily restorable from the Wenzel state with small energy inputs such as disturbances from wind or slight mechanical vibrations.

(3) It will be equally important to check whether the material can sustain cyclically applied large deformation during repeated switching. Although rubber and certain polymers can exhibit 400% elongation,[71] material selection for practical design of mechanically switchable surfaces can still be challenging since their failure strain could be substantially reduced under cyclic loading.

(4) The complexity in fabrication scheme can be a discouraging obstacle to realizing the proposed hierarchical design in the laboratory. In this respect, we wish to point out that the multilayer sinusoidal buckling design in the present paper is adopted mainly to make the development and presentation of our model self-consistent. In reality, certain foldable junctions like accordion structures may be simpler to realize in practical fabrication. It is quite exciting and encouraging that an increasing number of functional surfaces involving similar mechanisms and techniques have been successfully fabricated in the laboratory.[16,20,39,52,53,56] It is hoped that the present work can stimulate further studies on mechanically controllable multifunctional devices in the near future.

## 5. CONCLUSIONS

In this paper, an *n*-level wavy surface, which can be produced via sequential mechanical buckling upon release of prestrains in a multilayer system, was used as a model system to investigate the relationship among mechanical strain, surface morphology, wettability, and adhesion on hierarchical surfaces that can be mechanically switched between superhydrophilicity and superhydrophobicity. It is shown that such a surface possesses multiple function states, including superhydrophobic, hydrophobic, hydrophilic, and superhydrophilic states associated with wettability, as well as weak and strong sticky states associated with adhesion. All these functional states can be repeatedly and reversibly switched in a pure mechanical manner, by applying different levels of tensile strain on substrate. The theoretical study and experimental results in the literature indicate that hierarchical surfaces are a promising route to design multifunctional surfaces. Calculations of the critical pressure for CTW transition suggests that the self-cleaning state of the multifunctional surface should be robust enough to sustain extreme rainfall pressure found in nature, with great promises for a wide range of potential applications including water harvesting, oil spill cleanup, reversible adhesion, self-cleaning, environmental cleanup, microfluidics, micro- and nanofabrication, robotics, and biomedical engineering. The concepts of hierarchical design and mechanically controlled multifunctional devices proposed in this paper not only can help guide the fabrication of multifunctional devices, but may also motivate further research for mechanically controllable multifunctional devices.

## ■ ASSOCIATED CONTENT

### Supporting Information

Text and figures give the mathematical derivations and detailed discussions about eqs 6−10. This material is available free of charge via the Internet at http://pubs.acs.org.

## ■ AUTHOR INFORMATION

### Corresponding Author

*E-mail: Huajian_Gao@brown.edu.

## ■ ACKNOWLEDGMENTS

This work was supported by the A*STAR Visiting Investigator Program "Size Effects in Small Scale Materials" hosted at the Institute of High Performance Computing in Singapore.

## ■ REFERENCES

(1) Parker, A. R.; Lawrence, C. R. *Nature* **2001**, *414*, 33−34.
(2) Norgaard, T.; Dacke, M. *Front. Zool.* **2010**, *7*, 23−30.
(3) Zheng, Y.; Bai, H.; Huang, Z.; Tian, X.; Nie, F.-Q.; Zhao, Y.; Zhai, J.; Jiang, L. *Nature* **2010**, *463*, 640−643.
(4) Jernelov, A. *Nature* **2010**, *466*, 182−183.
(5) Williams, N. *Curr. Biol.* **2010**, *20*, R613−R614.
(6) Wang, D. A.; Wang, X. L.; Liu, X. J. E.; Zhou, F. *J. Phys. Chem. C* **2010**, *114*, 9938−9944.
(7) Kamperman, M.; Kroner, E.; del Campo, A.; McMeeking, R. M.; Arzt, E. *Adv. Eng. Mater.* **2010**, *12*, 335−348.
(8) Xia, F.; Jiang, L. *Adv. Mater.* **2008**, *20*, 2842−2858.
(9) Cheng, Z. J.; Feng, L.; Jiang, L. *Adv. Funct. Mater.* **2008**, *18*, 3219−3225.

(10) Reddy, S.; Arzt, E.; del Campo, A. *Adv. Mater.* **2007**, *19*, 3833−3837.
(11) Barthlott, W.; Neinhuis, C. *Planta* **1997**, *202*, 1−8.
(12) Sethi, S.; Ge, L.; Ci, L.; Ajayan, P. M.; Dhinojwala, A. *Nano Lett.* **2008**, *8*, 822−825.
(13) Bhushan, B.; Jung, Y. C.; Koch, K. *Philos. Trans. R. Soc. A* **2009**, *367*, 1631−1672.
(14) Blossey, R. *Nat. Mater.* **2003**, *2*, 301−306.
(15) Bhushan, B.; Ling, X. *J. Colloid Interface Sci.* **2009**, *329*, 196−201.
(16) Efimenko, K.; Finlay, J.; Callow, M. E.; Callow, J. A.; Genzer, J. *ACS Appl. Mater. Interfaces* **2009**, *1*, 1031−1040.
(17) Chunder, A.; Etcheverry, K.; Londe, G.; Cho, H. J.; Zhai, L. *Colloid Surf., A* **2009**, *333*, 187−193.
(18) Beebe, D. J.; Moore, J. S.; Yu, Q.; Liu, R. H.; Kraft, M. L.; Jo, B. H.; Devadoss, C. *Proc. Natl. Acad. Sci. U. S. A.* **2000**, *97*, 13488−13493.
(19) Gau, H.; Herminghaus, S.; Lenz, P.; Lipowsky, R. *Science* **1999**, *283*, 46−49.
(20) Lin, P. C.; Yang, S. *Soft Matter* **2009**, *5*, 1011−1018.
(21) Pugno, N. M. *Nano Today* **2008**, *3*, 35−41.
(22) Dai, Z. D.; Sun, J. R. *Prog. Nat. Sci.* **2007**, *17*, 1−5.
(23) Bhushan, B.; Ling, X. *J. Phys.: Condens. Matter* **2008**, *20*, 485009.
(24) Nosonovsky, M.; Bhushan, B. *J. Adhes. Sci. Technol.* **2008**, *22*, 2105−2115.
(25) Robinson, J. R.; Lee, V. H. L. *Controlled Drug Delivery-Fundamentals And Applications*, 2nd ed.; Marcel Dekker: New York, 1987.
(26) Autumn, K. *MRS Bull.* **2007**, *32*, 473−478.
(27) Autumn, K.; Liang, Y. A.; Hsieh, S. T.; Zesch, W.; Chan, W. P.; Kenny, T. W.; Fearing, R.; Full, R. J. *Nature* **2000**, *405*, 681−685.
(28) Autumn, K.; Sitti, M.; Liang, Y. C. A.; Peattie, A. M.; Hansen, W. R.; Sponberg, S.; Kenny, T. W.; Fearing, R.; Israelachvili, J. N.; Full, R. J. *Proc. Natl. Acad. Sci. U. S. A.* **2002**, *99*, 12252−12256.
(29) Hansen, W. R.; Autumn, K. *Proc. Natl. Acad. Sci. U. S. A.* **2005**, *102*, 385−389.
(30) Nosonovsky, M.; Bhushan, B. *Nano Lett.* **2007**, *7*, 2633−2637.
(31) Cortese, B.; D'Amone, S.; Manca, M.; Viola, I.; Cingolani, R.; Gigli, G. *Langmuir* **2008**, *24*, 2712−2718.
(32) Hui, C. Y.; Jagota, A. J.; Shen, L. L.; Rajan, A.; Glassmaker, N.; Tang, T. *J. Adhes. Sci. Technol.* **2007**, *21*, 1259−1280.
(33) Kim, S.; Sitti, M. *Appl. Phys. Lett.* **2006**, *89*, 261911.
(34) Lee, J. H.; Fearing, R. S.; Komvopoulos, K. *Appl. Phys. Lett.* **2008**, *93*, 191910.
(35) Greiner, C.; del Campo, A.; Arzt, E. *Langmuir* **2007**, *23*, 3495−3502.
(36) Xia, F.; Feng, L.; Wang, S. T.; Sun, T. L.; Song, W. L.; Jiang, W. H.; Jiang, L. *Adv. Mater.* **2006**, *18*, 432−436.
(37) Lim, H. S.; Han, J. T.; Kwak, D.; Jin, M. H.; Cho, K. *J. Am. Chem. Soc.* **2006**, *128*, 14458−14459.
(38) Riskin, M.; Basnar, B.; Chegel, V. I.; Katz, E.; Willner, I.; Shi, F.; Zhang, X. *J. Am. Chem. Soc.* **2006**, *128*, 1253−1260.
(39) Efimenko, K.; Rackaitis, M.; Manias, E.; Vaziri, A.; Mahadevan, L.; Genzer, J. *Nat. Mater.* **2005**, *4* (4), 293−297.
(40) Northen, M. T.; Greiner, C.; Arzt, E.; Turner, K. L. *Adv. Mater.* **2008**, *20*, 3905−3909.
(41) Lee, J.; Fearing, R. S. *Langmuir* **2008**, *24*, 10587−10591.
(42) Lee, H.; Lee, B. P.; Messersmith, P. B. *Nature* **2007**, *448*, 338−341.
(43) Gorb, S.; Varenberg, M.; Peressadko, A.; Tuma, J. *J. R. Soc. Interface* **2007**, *4*, 271−275.
(44) Jeong, H. E.; Kwak, M. K.; Suh, K. Y. *Langmuir* **2010**, *26*, 2223−2226.
(45) Cassie, A.; Baxter, S. *Trans. Faraday Soc.* **1944**, *40*, 546−551.
(46) Wenzel, R. N. *Ind. Eng. Chem.* **1936**, *28*, 988−994.
(47) Herminghaus, S. *Europhys. Lett.* **2000**, *52*, 165−170.
(48) Nosonovsky, M.; Bhushan, B. *Adv. Funct. Mater.* **2008**, *6*, 843−855.
(49) Yao, X.; Chen, Q. W.; Xu, L.; Li, Q. K.; Song, Y. L.; Gao, X. F.; Quere, D.; Jiang, L. *Adv. Funct. Mater.* **2010**, *20*, 656−662.
(50) Vajpayee, S.; Khare, K.; Yang, S.; Hui, C. Y.; Jagota, A. *Adv. Funct. Mater.* **2011**, *21*, 547−555.
(51) Neinhuis, C.; Barthlott, W. *Ann. Bot.* **1997**, *79*, 667−677.
(52) Khang, D. Y.; Jiang, H. Q.; Huang, Y.; Rogers, J. A. *Science* **2006**, *311*, 208−212.
(53) Jiang, H. Q.; Khang, D. Y.; Song, J. Z.; Sun, Y. G.; Huang, Y. G.; Rogers, J. A. *Proc. Natl. Acad. Sci. U. S. A.* **2007**, *104*, 15607−15612.
(54) Brau, F.; Vandeparre, H.; Sabbah, A.; Poulard, C.; Boudaoud, A.; Damman, P. *Nat. Phys.* **2011**, *7*, 56−60.
(55) Cai, S.; Breid, D.; Crosby, A. J.; Suo, Z.; Hutchinson, J. W. *J. Mech. Phys. Solids* **2011**, *59*, 1094−1114.
(56) Lin, P. C.; Vajpayee, S.; Jagota, A.; Hui, C. Y.; Yang, S. *Soft Matter* **2008**, *4*, 1830−1835.
(57) Chan, E. P.; Smith, E. J.; Hayward, R. C.; Crosby, A. J. *Adv. Mater.* **2008**, *20*, 711−716.
(58) Rahmawan, Y.; Moon, M.-W.; Kim, K.-S.; Lee, K.-R.; Suh, K.-Y. *Langmuir* **2010**, *26*, 484−491.
(59) Genzer, J.; Groenewold, J. *Soft Matter* **2006**, *2*, 310−323.
(60) Chen, X.; Hutchinson, J. W. *J. Appl. Mech.* **2004**, *71*, 597−603.
(61) Huang, R. *J. Mech. Phys. Solids* **2005**, *53*, 63−89.
(62) Huang, Z. Y.; Hong, W.; Suo, Z. *J. Mech. Phys. Solids* **2005**, *53*, 2101−2118.
(63) Quere, D. *Rep. Prog. Phys.* **2005**, *68*, 2495−2532.
(64) Kim, S.; Cheung, E.; Sitti, M. *Langmuir* **2009**, *25*, 7196−7199.
(65) Lafuma, A.; Quere, D. *Nat. Mater.* **2003**, *2*, 457−460.
(66) Su, Y.; Ji, B.; Zhang, K.; Gao, H.; Huang, Y.; Hwang, K. *Langmuir* **2010**, *26*, 4984−4989.
(67) Wagner, P.; Furstner, R.; Barthlott, W.; Neinhuis, C. *J. Exp. Bot.* **2003**, *54*, 1295−1303.
(68) Erpul, G.; Norton, L. D.; Gabriels, D. *CATENA* **2002**, *47*, 227−243.
(69) Boreyko, J. B.; Chen, C.-H. *Phys. Rev. Lett.* **2009**, *103*, 174502.
(70) Song, J.; Jiang, H.; Liu, Z. J.; Khang, D. Y.; Huang, Y.; Rogers, J. A.; Lu, C.; Koh, C. G. *Int. J. Solids Struct.* **2008**, *45*, 3107−3121.
(71) Volynskii, A. L.; Bazhenov, S.; Lebedeva, O. V.; Bakeev, N. F. *J. Mater. Sci.* **2000**, *35*, 547−554.